A CONDITIONAL RANDOM FIELD MODEL FOR TRACKING IN DENSELY PACKED CELL STRUCTURES

*Anirban Chakraborty, Amit Roy-Chowdhury**

Department of Electrical Engineering, University of California, Riverside, USA

ABSTRACT

Automated tracking of plant and animal cells in time lapse live-imaging datasets of developing multicellular tissues is required for quantitative, high throughput analysis of cell division, migration and cell growth. In this paper, we present a novel cell tracking method that exploits the tight spatial topology of neighboring cells in a multicellular field as contextual information and combines it with physical features of individual cells for generating reliable cell lineages. The 2D image slices of multicellular tissues are modeled as CRFs and spatio-temporal cell to cell correspondences are obtained by performing inference on this CRF using loopy belief propagation. We present results on a (3D+t) confocal image stack of Arabidopsis shoot meristem and show that the method can handle many visual analysis challenges associated with such cell tracking problems, viz. poor feature quality of individual cells, low SNR in parts of images, variable number of cells across slices and cell division detection.

***Index Terms*—** Cell tracking, Conditional Random Field, Spatial context, Live cell imaging.

1. INTRODUCTION

In developmental biology, the causal relationship between cell growth patterns and gene expression dynamics has been one of the major topics of interest. A proper quantitative analysis of the cell growth and division patterns in both the plant and the animal tissues has remained mostly elusive so far. Towards this goal, with the advancements in microscopy and other imaging techniques, time lapse videos are being collected to quantify the behavior of hundreds of cells in a tissue over multiple days. For high-throughput analysis of these large volumes of image data, development of fully automated image analysis pipelines are becoming necessities, thereby giving rise to many new automated visual analysis challenges.

Automated cell tracking with cell division detection is one of the major components of all such pipelines (such as [1]). The computational challenges related to a robust design of cell tracker come from multiple sources such as variable number of cells in the field of view (FoV), deformation of cell shapes, complex topologies of cell clusters, low SNR in the images, etc. In this paper, we present an automated visual tracker for cells tightly packed in developing multilayer tissues. This calls for developing strategies for *temporal* associations of the cells. Moreover, since at every time point of observation a cell could be imaged across multiple spatial planes, the tracking method must be capable of finding correspondences in the *spatial* direction as well. Beyond these, the tracker has to be able to detect cell divisions, detect new cells as the deeper layers of the tissues are imaged, differentiate between cells in a close neighborhood sharing similar physical features and generate correct matches in presence of low SNR.

There has been some work on automated tracking and segmentation of cells in time-lapse images, for both plants and animals. One of the well-known approaches for segmenting and tracking cells is based on evolution of active contours [2, 3, 4, 5, 6]. But this method is not suitable for tracking where all the cells are in close contact with each other and share very similar physical features, nor is there any reported result on spatial correspondence. The Softassign method uses the information on point location to simultaneously solve both the problem of global correspondence as well as the problem of affine transformation between two time instants iteratively [7, 8]. However, these methods are more suitable for aligning global features than finding correspondences between non-uniformly growing individual cells. Although [8] presents a sample result on a shoot meristem without validating against ground truth, it is not enough to evaluate the accuracy of this method on a typical 4D confocal data.

Besides the aforementioned approaches, tracking based on association between detections such as [9, 10, 11] has shown good performance on time-lapse images. However, these methods perform well when the feature quality or the underlying motion model is reliable. We are looking at a more challenging problem, where the features extracted from each cell may not be reliable or discriminating enough (such as cell shape/area which is often stereotypical even in a small cluster).

In [12, 13], a spatio-temporal tracking algorithm for Arabidopsis SAM was proposed, where relative positional infor-

*Corresponding author, email: amitrc@ee.ucr.edu

This work was partially supported by NSF grant IIS-0712253.

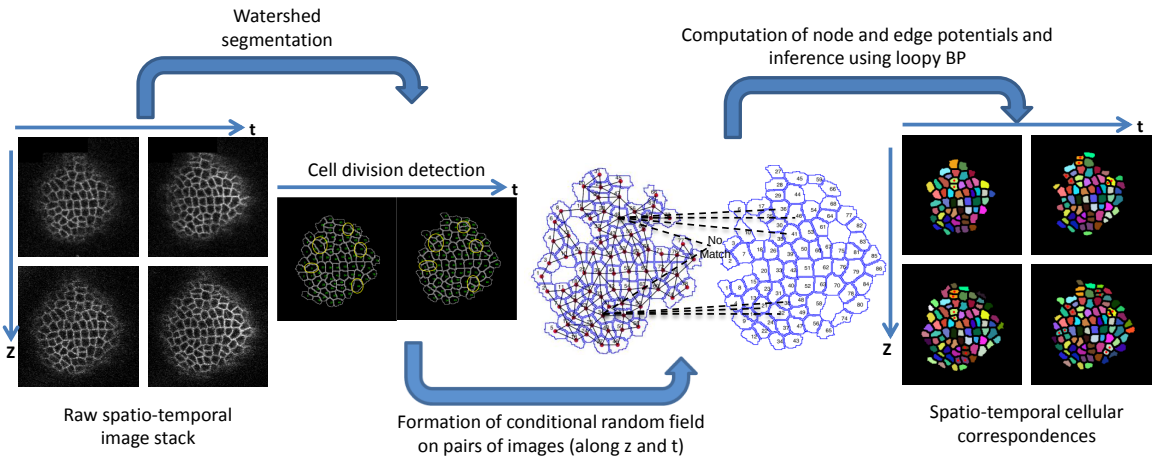

Fig. 1. Proposed cell tracking framework - different sequential components in the proposed method.

mation of neighboring cells was used to generate unique features for each cell. However, this method employs an iterative search strategy by growing correspondence from a *seed* cell pair which tends to accumulate error and can throw the tracker off for cells spatially distant from the seed.

In this work, we propose to solve the spatio-temporal tracking problem as a graph inference problem. To track cells between two image slices consecutive in time or space, we build a graph on one of the images with individual cells as the nodes and neighboring nodes sharing an undirected edge between them. We further define a Conditional Random Field (CRF) on the graph, the probable states of each node being the candidate cell correspondences from the next image. A distance defined on the physical features extracted from a cell and that of each of its candidate matches is used to constitute the node potential. The spatial context is modeled on each of the edges based on the relative location of the cell and its neighbors by utilizing the tight spatial topology of the cell clusters. We obtain the correspondences by maximizing the marginal distribution computed at each node (cell). The approximate marginals are obtained by a Loopy Belief Propagation scheme. The overall tracking pipeline is shown in Fig. 1.

2. SPATIO-TEMPORAL CELL TRACKING METHOD

2.1. Pre-processing: Segmentation and Registration

The input to our cell tracking system is a (3D+t) image stack, which is a collection of 2D image slices along the depth of a tissue and along multiple time points of observation. A 2D segmentation technique (such as Watershed as in [14]) is employed to segment out individual 2D cell cross sections on each of the image slices. The 3D stacks are further registered temporally using a 'local graph' based registration scheme [15].

2.2. Graph Formation on 2D Segmentations

Let us define the problem to be to find correspondences between the cells in two confocal image slices I_G and I_M. The Watershed segmentation of I_G and I_M produces two sets of cell segments Ω_G and Ω_M respectively and $\mathcal{O} = \Omega_G \cup \Omega_M$. For temporal tracking, we first detect if some cells form I_G have divided into pairs of cells in I_M following the method described in Sec. 2.4 and remove the parent cells that have undergone division from Ω_G and the divided children from Ω_M. The graph and the candidate states of each node of the graph are thereafter formed using the remaining subsets of cells V_G and V_M containing N_G and N_M cells respectively, i.e. the remaining cells $v_G^1, v_G^2, \cdots v_G^{N_G} \in V_G \subseteq \Omega_G$ and $v_M^1, v_M^2, \cdots v_M^{N_M} \in V_M \subseteq \Omega_M$. The graph is built on I_G and the set of nodes V_G is same as the set of segmented cells sans the cells undergoing division. Any two nodes v_G^i and v_G^j will have an edge between them if v_G^i and v_G^j are spatial neighbors (Fig. 1). For tightly packed cluster of cells, v_G^i and v_G^j are neighbors if they share a common boundary or if they are within close spatial proximity for non-compactly arranged cellular tessellations.

2.3. Determination of Candidate States For Every Node

Each node in the graph, corresponding to a cell slice v_G^i represents a random variable x_i that can take a label s_k^i from the set S_G^i which is the set of K closest segments in the slice I_M around the point $\mathbf{c}_G^i$, the centroid of v_G^i on I_G. Now, we add an additional label s_0^i to the candidate set S_G^i that represents the case where the cell slice v_G^i is not imaged in the slice I_M. Thus, the complete set of candidate states becomes $S_G^i = \{s_0^i, s_1^i, \cdots s_K^i\}$.

2.4. Cell Division Detection

To detect cell divisions before forming the graph g_G in temporal tracking, we first compute the candidate sets C_G^i in I_M for a segmented cell slice $\omega_G^i \in \Omega_G$ following similar method as in Sec. 2.3. Next we form all possible pairs of the candidate cells from C_G^i that share a boundary as in $D_G^i = \left\{(cd_p^i,\ cd_q^i)\ s.t.\ cd_p^i \in nbor(cd_q^i) \text{ and } cd_p^i, cd_q^i \in C_G^i\right\}$. Now, if the cell ω_G^i has divided into two children cells cd_p^i and cd_q^i, then ideally the shape of ω_G^i should be very similar to the combined shape of cd_p^i and cd_q^i, taken together (i.e. to the shape of $(cd_p^i \cup cd_q^i)$) and each of cd_p^i and cd_q^i would be approximately half the size of ω_G^i. Motivated by this physical property associated with cell division, we compute a set of distances as $d(\omega_G^i, D_G^i) = \{\frac{1}{t_1} MHD(b(\omega_G^i), b(cd_p^i \cup cd_q^i)) + \frac{1}{t_2}\left[\left|\frac{1}{2} - \frac{area(cd_p^i)}{area(\omega_G^i)}\right| + \left|\frac{1}{2} - \frac{area(cd_q^i)}{area(\omega_G^i)}\right|\right]$ for all $(cd_p^i, cd_q^i) \in D_G^i\}$, where b is the set of boundary points on a shape recomputed with respect to its centroid and MHD is the modified Hausdorff distance. If $\min d(\omega_G^i,\ D_G^i) \leq 1$, then it is inferred that the cell ω_G^i has divided into the cell pair in D_G^i for which this minimum is obtained. The values of the parameters t_1 and t_2 are learned from a small training set.

2.5. Conditional Random Field Modeling

Let the set of random variables associated with V_G be $X = \{x_1, x_2, \cdots x_{N_G}\}$, which are to be estimated given the observation I_M. These random variables correspond to the state of each node in the graph and the support for each of these variables is the candidate set as discussed in Sec. 2.3. These variables are modeled as a Conditional Random Field (CRF) and the node and edge potential functions associated with this CRF are computed via the following techniques.

2.6. Computation of Observation/Node Potential:

The node potential is defined on every node of the graph, which is the likelihood on the label taken by a node belonging to V_G, given the observation $\mathcal{O}$. This potential is computed independently for each node based on its shape similarities with each of its candidates.

For measuring similarities between cell shapes, we generate a shape histogram descriptor for each of the cells, which is very similar to one of the methods described in [16]. Let the shape histogram associated with the cell slice v_G^i be h_G^i and that with the candidate slice s_j^i be h_M^j (as $s_j^i \in V_M$). We computed the K-L divergence (KLD) between h_G^i and h_M^j which gives us a distance measure between these two cell slices and suppose it is represented as $d^i\left(v_G^i, s_j^i\right)$. The corresponding node potential for each node is

$$\phi_i\left(x_i = s_j^i; \mathcal{O}\right) \ = \ \exp\left(-d^i(v_G^i,\ s_j^i)/\lambda\right)\ \forall j = 1, 2 \cdots K \tag{1}$$

$$\phi_i\left(x_i = s_0^i; \mathcal{O}\right) = 1 - \max_j \left\{\phi_i\left(x_i = s_j^i; \mathcal{O}\right), j = 1, \cdots K\right\} \tag{2}$$

2.7. Computation of Spatial Context / Edge Potential:

This potential function is defined on edges connecting pairs of neighboring nodes and is representative of the conditional distribution $P(x_j|x_i, \mathcal{O})$. The computation of the potential function depends on the fact that if two neighboring cells v_G^i and v_G^j are tracked to two cell slices v_M^p and v_M^q, then the relative position of v_G^j with respect to v_G^i should be very similar to that of v_M^q and v_M^p. As a result, if v_G^i is tracked to v_M^p then the probability that v_G^j corresponds to v_M^q gets boosted if $\mathbf{c}_G^j - \mathbf{c}_G^i \ \approx \ \mathbf{c}_M^q - \mathbf{c}_M^p$, where $\mathbf{c}_G^i, \mathbf{c}_G^j, \mathbf{c}_M^p, \mathbf{c}_M^q$ be the centroids of $v_G^i, v_G^j, v_M^p, v_M^q$ respectively.

Clearly, the additional evidences for matching two cell slices in I_G and I_M come in the form of local neighborhood structure based contextual information. Thus, the contextual transition potentials between any two nodes v_G^i and v_G^j taking non-zero states can be expressed as a function of the shift between the relative positions of those nodes

$$\begin{aligned}&\psi_{i,j}\left(x_i = s_p^i, x_j = s_q^j; \mathcal{O}\right)\\ &\quad = \exp\left\{-\gamma\|(\mathbf{c}_G^j - \mathbf{c}_G^i) - (\mathbf{c}_M^{s_q^j} - \mathbf{c}_M^{s_p^i})\|_2\right\}\end{aligned} \tag{3}$$

$\forall p, q = 1, 2, \cdots K$, where $s_p^i \in S_G^i, s_q^j \in S_G^j$.

Now, the transition potentials must also incorporate the case where one of the cells is not tracked and its neighboring cell is matched to one of the cells in the next slice or not matched to any cell. This potential can be taken as uniform over the support of the neighboring cell.

$$\psi_{i,j}\left(x_i = s_0^i,\ x_j = s_q^j; \mathcal{O}\right) \ = \ \frac{1}{K+1}\ \forall q = 0, 1, \cdots K\ . \tag{4}$$

Finally, when v_G^i has a match in the next spatial or temporal image slice I_M, but its neighbor v_G^j does not, then the corresponding edge potential entries become

$$\begin{aligned}&\psi_{i,j}\left(x_i = s_p^i,\ x_j = s_0^j; \mathcal{O}\right)\\ &= 1 - \max_q \left\{\psi_{i,j}\left(x_i = s_p^i, x_j = s_q^j; \mathcal{O}\right),\ q = 1, 2, \cdots K\right\}\end{aligned} \tag{5}$$

for $p \neq 0$.

2.8. Inference: Loopy Belief Propagation

The next step is to do the inference on the CRF, which involves the computation of the marginal probability distributions for the states x_i of each node $v_G^i \in V_G$, given the observations $\mathcal{O}$. For computation of the marginals at each node, we

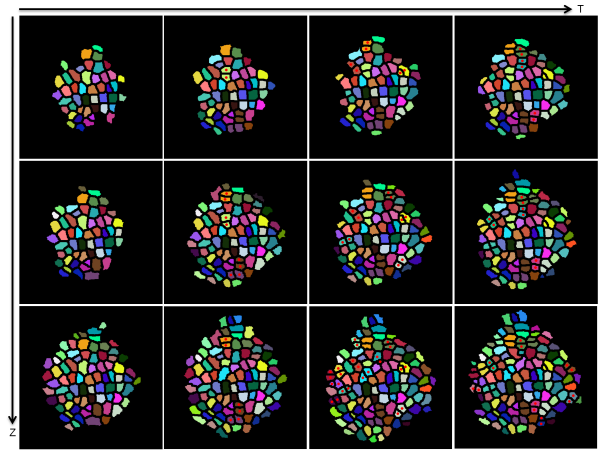

Fig. 2. Results showing combined spatio-temporal tracking on Arabidopsis SAM dataset (best seen in color).

choose to use a very popular iterative *message-passing* algorithm known as *Loopy Belief Propagation* (LBP) based on the *Sum-Product* algorithm [17]. If LBP converges at iteration L, the estimated marginals at each node would be $P^{(L)}(x_i;\mathcal{O})$ and the MAP estimate for the most likely state is computed as $\hat{x_i} = \arg_{x_i} \max P^{(L)}(x_i;\mathcal{O})$. This optimum state corresponds to either the 'no-match' case or a specific cell in I_M.

3. TRACKING RESULTS AND ANALYSIS

We have tested our proposed cell tracking method on a 4D confocal stack of Arabidopsis shoot apical meristem (SAM) that showcases all the challenges associated with any spatio-temporal cell tracking problem in a tightly packed multilayer tissue. The 3D structure of the tissue is imaged using single-photon confocal laser scanning microscope, thereby generating a series of serial optical image slices of cells (only the cell-walls are visible). Observations are taken every three hours to yield a (3D+t) confocal stack.

We perform spatial cell tracking across the depth of the 3D confocal image stacks and combine them with temporal tracking of the same cells across time. In Fig. 2, we sample three consecutive spatial slices from confocal stacks at 4 different time points (at $12^{th}, 15^{th}, 18^{th}$ and 21^{st} hours of observation) and the tracking result for them are shown. The 2D slices coming from the same 3D cell are correctly tracked for all the cells across 4 different time instants and are marked with the same color. The children cells after division are marked by red dots. It can be observed that slices of new cells appear as we go deeper into the tissue and as expected, they are not matched to any cell from the slice above.

The complete tracking result on the dataset (12 time points and 7 slices at each time point) is summarized quantitatively in Table 1. TP corresponds to the cases where two cell

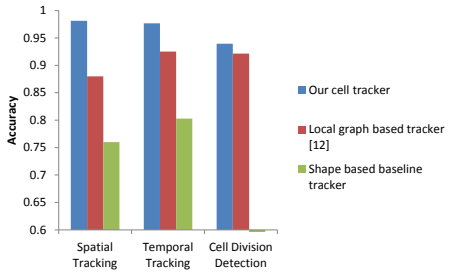

Fig. 3. Quantitative comparison of tracking accuracies obtained by proposed method, method in [12] and the baseline tracker on the entire dataset.

Table 1. Tracking Result Summary

	TP	FP	TN	FN
Spatial	86%	0.25%	12.13%	1.62%
Temporal	83%	0%	14.66%	2.34%
Division	31/33	0	-	2/33

slices are correctly matched either in space or time. When cell slices from two different cells are incorrectly matched together, it falls under FP. When the tracker fails to pick up a correct correspondence, it is represented by FN and its opposite case is tabulated under TN. In both spatial and temporal tracking, the accuracy is more than 97%.

A full quantitative comparison of tracking accuracies obtained by proposed method, method in [12] and the baseline tracker on the entire dataset is presented in Fig. 3. We designed the baseline tracker on the same local cell shape features as used to compute the node potentials in Sec. 2.6 and the tracker associates cell slices across images using 'Hungarian algorithm'. It can be observed from Fig. 3 that our proposed method substantially outperforms both [12] and the baseline tracker, especially in spatial tracking. We have also compared the results obtained by the proposed method and the method in [12] in detecting cell divisions and observed that the proposed method marginally outperforms [12].

4. CONCLUSION

We have presented a method for automatically tracking individual cells in closely packed developing multilayer tissues. We observed that cells in a close cluster in the tissue can have very similar image features and hence we leveraged upon the local spatial geometric structure and topology of the relative positions of the neighboring cells to robustly track growing cells in the tissue in presence of imaging noise. Future work would include the integration of this spatio-temporal tracking method with other image analysis components such as a cell resolution 3D reconstruction method [18] to design a complete 4D image analysis pipeline.

5. REFERENCES

[1] Romain Fernandez, Pradeep Das, Vincent Mirabet, Eric Moscardi, Jan Traas, Jean-Luc Verdeil, Gregoire Malandain, and Christophe Godin, "Imaging plant growth in 4d: robust tissue reconstruction and lineaging at cell resolution," *Nature Methods*, vol. 7, no. 7, pp. 547–553, 07 2010.

[2] O. Dzyubachyk, W.A. Van Cappellen, J. Essers, W.J. Niessen, and E. Meijering, "Advanced level-set-based cell tracking in time-lapse fluorescence microscopy," *Medical Imaging, IEEE Transactions on*, vol. 29, no. 3, pp. 852–867, 2010.

[3] Kang Li and Takeo Kanade, "Cell population tracking and lineage construction using multiple-model dynamics filters and spatiotemporal optimization," in *Proceedings of the 2nd International Workshop on Microscopic Image Analysis with Applications in Biology*, 2007.

[4] Kang Li, Mei Chen, Takeo Kanade, Eric Miller, Lee Weiss, and Phil Campbell, "Cell population tracking and lineage construction with spatiotemporal context," *Medical Image Analysis*, vol. 12, no. 5, pp. 546 – 566, 2008.

[5] Dirk R. Padfield, Jens Rittscher, Nick Thomas, and Badrinath Roysam, "Spatio-temporal cell cycle phase analysis using level sets and fast marching methods.," *Medical Image Analysis*, vol. 13, no. 1, pp. 143–155, 2009.

[6] A. Dufour, V. Shinin, S. Tajbakhsh, N. Guillen-Aghion, J. C. Olivo-Marin, and C. Zimmer, "Segmenting and tracking fluorescent cells in dynamic 3-D microscopy with coupled active surfaces," *IEEE Transactions on Image Processing*, vol. 14, no. 9, pp. 1396–1410, 2005.

[7] Haili Chui and Anand Rangarajan, "A new algorithm for non-rigid point matching," in *in CVPR*, 2000, pp. 44–51.

[8] Victoria Gor, Michael Elowitz, Tigran Bacarian, and Eric Mjolsness, "Tracking cell signals in fluorescent images," *IEEE Computer Society Conference on Computer Vision and Pattern Recognition Workshops*, vol. 0, pp. 142, 2005.

[9] Nezamoddin N. Kachouie, Paul Fieguth, John Ramunas, and Eric Jervis, "Probabilistic model-based cell tracking," *International Journal of Biomedical Imaging*, 2006.

[10] Thiagalingam Kirubarajan, Yaakov Bar-Shalom, and Krishna R. Pattipati, "Multiassignment for tracking a large number of overlapping objects," *IEEE Trans. on Aerospace and Electronic Systems*, vol. 37, no. 1, pp. 2–21, 2001.

[11] Ryoma Bise, Zhaozheng Yin, and Takeo Kanade, "Reliable cell tracking by global data association," in *IEEE International Symposium on Biomedical Imaging: From Nano to Macro*, 2011, pp. 1004–1010.

[12] Min Liu, Ram Kishor Yadav, Amit Roy-Chowdhury, and G. Venugopala Reddy, "Automated tracking of stem cell lineages of arabidopsis shoot apex using local graph matching," *Plant journal, Oxford, UK*, vol. 62, pp. 135–147, 2010.

[13] Min Liu, Anirban Chakraborty, Damanpreet Singh, Ram Kishor Yadav, Gopi Meenakshisundaram, G Venugopala Reddy, and Amit Roy-Chowdhury, "Adaptive cell segmentation and tracking for volumetric confocal microscopy images of a developing plant meristem," *Molecular Plant*, vol. 4, no. 5, pp. 922–31, 2011.

[14] Katya Mkrtchyan, Damanpreet Singh, Min Liu, G. Venugopala Reddy, Amit K. Roy Chowdhury, and M. Gopi, "Efficient cell segmentation and tracking of developing plant meristem," in *IEEE International Conference on Image Processing*, 2011, pp. 2165–2168.

[15] Katya Mkrtchyan, Anirban Chakraborty, and Amit K. Roy-Chowdhury, "Automated registration of live imaging stacks of arabidopsis," in *Biomedical Imaging (ISBI), 2013 IEEE 10th International Symposium on*, 2013, pp. 672–675.

[16] Mihael Ankerst, Gabi Kastenmüller, Hans-Peter Kriegel, and Thomas Seidl, "3d shape histograms for similarity search and classification in spatial databases," in *Proceedings of the 6th International Symposium on Advances in Spatial Databases*, 1999, pp. 207–226.

[17] Frank R. Kschischang, Brendan J. Frey, and Hans-Andrea Loeliger, "Factor graphs and the sum-product algorithm," *IEEE Transactions on Information Theory*, vol. 47, pp. 498–519, 1998.

[18] Anirban Chakraborty, Mariano M. Perales, G. Venugopala Reddy, and Amit K. Roy-Chowdhury, "Adaptive geometric tessellation for 3d reconstruction of anisotropically developing cells in multilayer tissues from sparse volumetric microscopy images," *PLoS ONE*, vol. 8, no. 8, pp. e67202, 08 2013.